JACS
JOURNAL OF THE AMERICAN CHEMICAL SOCIETY
Communication
pubs.acs.org/JACS

Postsynthetic Functionalization of a Hollow Silica Nanoreactor with Manganese Oxide-Immobilized Metal Nanocrystals Inside the Cavity

Soo Min Kim,[†] Mina Jeon,[†] Ki Woong Kim,[‡] Jaiwook Park,[†] and In Su Lee*[,†]

[†]Department of Chemistry, Pohang University of Science and Technology (POSTECH), Gyeogbuk 790-784, Korea
[‡]Department of Applied Chemistry, Kyung Hee University, Gyeonggi-do 446-701, Korea

Supporting Information

ABSTRACT: A postsynthetic protocol of functionalizing the preformed hollow nanoparticles with metal nanocrystals was developed based on galvanic replacement reaction on the Mn_3O_4 surface inside the cavity. The developed protocol produced hollow nanoreactor systems, in which a high density of ultrafine catalytic nanocrystals of a range of noble metals, such as Pd, Pt, Rh, and Ir and their alloys, are dispersively immobilized on an interior surface enclosed by a selectively permeable silica shell. The fabricated hollow nanoreactor exhibited highly enhanced activity, selectivity, and recyclability in catalyzing the oxidation of hydrosilanes, which are attributable to the synergistic combination of the porous silica nanoshell and the oxide-immobilized catalyst system.

Hollow inorganic nanoparticles, which have an interior cavity enclosed by an inorganic shell of nanosized thickness, have recently been receiving considerable attention because of their distinct characteristics that are advantageous for a variety of biomedical and catalytic applications.[1] Their hollow interior structure can be used to selectively encapsulate and release guest molecules and carry the high payload of the functional molecules on the large surface area, which therefore enriches their potential in the emerging fields such as nanoreactors,[2] drug delivery vehicles,[3] contrast agents for molecular imaging,[4] and energy and gas storage materials.[5] In particular, hollow nanostructures that encapsulate catalytic species inside the permeable porous shell of chemically inert materials are promising candidates for nanoreactors that efficiently catalyze the chemical reactions of selected molecules while preserving the exposed surface area of the entrapped catalysts even under harsh reaction conditions or during the recycling process.[6,7] To increase the potential applications of such nanoparticles in nanoreactors, it is essential to develop a new method for functionalizing the internal cavity, which allows chemical reactions to occur within the protective void space. Several effective methods have been proposed to incorporate catalytic nanoparticles inside the cavity of the hollow nanoparticles through various approaches, including the template etching process and methods based on the Ostwald ripening, galvanic replacement, and nanoscale Kirkendall effects.[8] Most of the above-mentioned methods are used to produce yolk-shell nanostructures by selectively removing a part of a priorly synthesized core−shell nanostructure, which leaves a single metal nanoparticle core inside the newly generated void space.[9] In this context, we report our research intended to exploit a postsynthetic modification method to functionalize preformed void spaces of the hollow nanoparticles, which might be more desirable for enhancing the variability in the number and the nature of entrapped catalytic nanoparticles. For this purpose, we attempted to further develop our recent discovery that Pd and Pt nanocrystals are spontaneously deposited on the Mn_3O_4 surface from their precursor solutions, through the galvanic replacement process without the use of any additional reducing agents.[10] It was envisioned that if this process is properly taking place in the interior cavity, it could be a simple and efficient method for decorating the interior surface of the preformed hollow nanostructure with large multiple numbers of catalytic nanoparticles, which are more advantageous for catalytic applications than is a yolk-shell nanostructure with a single large core.[11]

Herein, we report a postsynthetic functionalization protocol based on galvanic replacement at the Mn_3O_4 surface, which leads to the high-density deposition of ultrafine metal nanoparticles on a Mn_3O_4-layer-coated interior surface of the hollow silica nanosphere (Scheme 1). The hollow nanoreactor

Scheme 1. Protocol of Functionalizing the Interior Surface of a Hollow Silica Nanoparticle

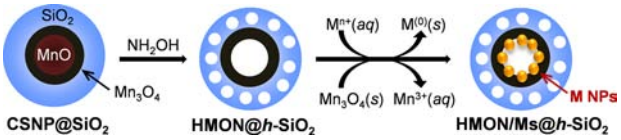

fabricated using the proposed method exhibited highly enhanced activity, selectivity, and recyclability in catalyzing the hydrolytic oxidation of silanes, which are attributable to the synergistic combination of the porous silica nanoshell and the oxide-immobilized catalyst system. We also demonstrated the broad scope of the proposed protocol to diversify the functions of the hollow nanoreactor by introducing various catalytic metal species, including Pd, Pt, Rh, Ir, and their alloys.

The hollow silica nanosphere with a Mn_3O_4 layer on the interior surface, **HMON@*h*-SiO$_2$**, which was used as a platform in this study, was prepared using a recently developed procedure involving silica encapsulation of a MnO−Mn_3O_4

Received: August 13, 2013
Published: October 8, 2013

   dx.doi.org/10.1021/ja4083792 | J. Am. Chem. Soc. 2013, 135, 15714−15717

core−shell nanoparticle (CSNP), followed by treatment with hydroxylamine solution for etching the MnO core and rendering the silica porous.[12] The resultant **HMON@*h*-SiO$_2$** obtained from 16 (±1) nm-sized CSNP consisted of a porous and hollow silica nanoshell with an 8 (±1) nm diameter cavity and a 4.3 (±0.5) nm Mn_3O_4 layer on the interior surface (Figure 1a). To induce Pd deposition on the Mn_3O_4 layer,

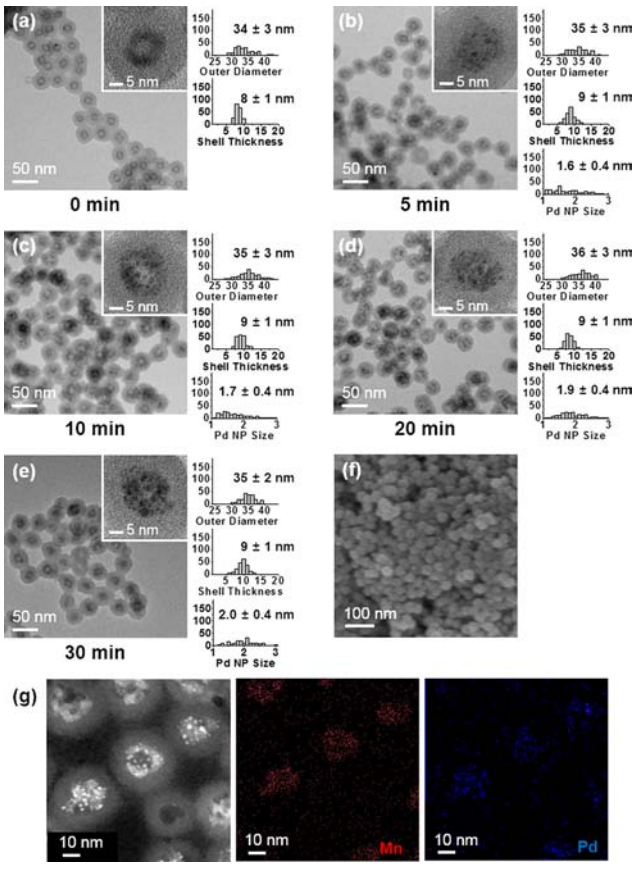

Figure 1. TEM and HRTEM (inset) images of (a) **HMON@*h*-SiO$_2$** having a shell thickness of 8.5 nm and samples obtained after its reaction with Na_2PdCl_4 at pH 2.4 for (b) 5, (c) 10, (d) 20, and (e) 30 min. Histograms are showing the outer diameter and the thickness of the silica shell and the size of the deposited Pd nanocrystals. (f) SEM and (g) STEM-HAADF image and elementary maps of **HMON/Pds@*h*-SiO$_2$** obtained after 30 min reaction.

HMON@*h*-SiO$_2$ was immersed in an aqueous solution of Na_2PdCl_4 at 70 °C by following a procedure that was used for the surfactant free Mn_3O_4 nanoparticle (**Sf-MON**).[10] The results of initial experiments revealed that the thickness of the silica shell, which varies between 7.5 and 12.5 nm with the duration of the silica encapsulation procedure, is a critical factor in the reaction of $PdCl_4^{2-}$ and Mn_3O_4. Therefore, **HMON@*h*-SiO$_2$** with a shell thickness >11.7 (±0.9) nm, which was prepared through silica encapsulation for longer than 12 h, did not generate any reduced Pd species from the solution, presumably because the reducing Mn_3O_4 layer was shielded by a relatively thicker and denser silica shell (Figure S1).[13] In contrast, immersion of **HMON@*h*-SiO$_2$**s with shell thicknesses of 7.5, 8.5, and 10.3 nm caused gradual darkening of the suspension color, indicating the reduction of $PdCl_4^{2-}$ into metallic Pd species, and resulted in translucent dark-brown suspensions within 30 min. The formation of tiny Pd nanoparticles, which accompanies the partial dissolution of the Mn_3O_4 layer, was identified by TEM observations of the resulted particles. The control experiment with hollow silica nanoparticles prepared from **HMON@*h*-SiO$_2$** by dissolving Mn_3O_4 did not give any Pd species, which confirmed that the reduction of $PdCl_4^{2-}$ proceeded through the galvanic reaction with Mn_3O_4 inside the permeable silica shell (Figure S2).

The results of TEM analyses also revealed that a low pH, which may prevent the deposition and precipitation of Pd^{2+} species on the silica surface, is essential for the growth of Pd nanocrystals exclusively on the interior surface.[14] Thus, the reaction of **HMON@*h*-SiO$_2$** having a shell thickness of 8.5 nm with $PdCl_4^{2-}$ at pH 2.4 led to Pd deposition on the Mn_3O_4 layer on the interior surface, while the treatment at pH > 2.5 led to Pd growth outside the silica shell (Figure S3). TEM images recorded at different instances during the reaction at pH 2.4 showed that tiny Pd nanocrystals with an average size of 1.6 (±0.4) nm began to emerge on the Mn_3O_4 layer at 5 min (Figure 1b). As the reaction proceeded, slightly larger Pd nanocrystals were additionally deposited, which is consistent with the previous observation during the galvanic replacement reaction on **Sf-MON** (Figure 1c,d). Therefore, the SEM, TEM, and STEM elemental mapping images obtained after a reaction time of 30 min revealed the formation of the targeted **HMON/Pds@*h*-SiO$_2$** (Figure 1e−g). In this product, 2.0 (±0.4) nm-sized Pd nanocrystals were densely and dispersively deposited on the partially dissolved Mn_3O_4 layer, on the internal surface of a porous and hollow silica nanoshell, whose inner and outer diameters were 16 (±2) and 35 (±2) nm, respectively. The nitrogen adsorption/desorption isotherm analysis shows that the resulted **HMON/Pds@*h*-SiO$_2$** has 287 m^2/g of a BET surface area and micropores in the silica shell with a bimodal size distribution each centered at 0.7 and 1.4 nm (Figure S4). The Pd and Mn contents of **HMON/Pds@*h*-SiO$_2$** were determined to be 2.5 and 5.1 wt %, respectively, by using inductively coupled plasma atomic emission spectroscopy (ICP-AES). Thus, **HMON/Pds@*h*-SiO$_2$**, in which an oxide-immobilized nanocrystalline-catalyst system is confined to the void space protected by a selectively permeable silica shell, can efficiently catalyze the transformation of the selected molecules and can be recycled many times without loss of activity.

In order to verify the effectiveness of **HMON/Pds@*h*-SiO$_2$** as a nanoreactor, we investigated its catalytic performance in the hydrolytic oxidation of hydrosilanes (**1**), which is known to be facilitated by noble metal-based catalysts (Table 1).[15] In the trial reaction of dimethylphenylsilane (**1b**) and water (3 equiv) with 1 mol % of **HMON/Pds@*h*-SiO$_2$** in acetone at room temperature (rt), dimethylphenylsilanol (**2b**) was afforded as the sole product in quantitative yield within 30 min (entry 3). In contrast, the control reaction with the same wt% of **HMON@*h*-SiO$_2$** afforded only 2% conversion yield for 24 h, implying that the Pd nanocrystals inside the silica shell are responsible for the catalytic activity of the **HMON/Pds@*h*-SiO$_2$**. The turnover number (TON) of the **HMON/Pds@*h*-SiO$_2$** estimated based on the conversion yield with 0.0005 mol % of the catalyst for over 6 h was >198 000, which is highest among those reported so far for silane oxidation reactions with heterogeneous catalysts.[15a] The control reactions by using commercialized $Pd/CaCO_3$, Pd/Al_2O_3, and Pd/C catalysts, which immobilize 6 (±2), 3.7 (±0.6), and 3.2 (±0.6) nm-sized Pd nanoparticles, respectively, gave only 10 000−36 000 of TONs, which confirms the highly enhanced activity of the **HMON/Pds@*h*-SiO$_2$** (Figure S5). Although the exact

dx.doi.org/10.1021/ja4083792 | J. Am. Chem. Soc. 2013, 135, 15714−15717

Table 1. Oxidation of Hydrosilanes into Silanols with HMON/Pds@*h*-SiO$_2$ as a Catalyst[a]

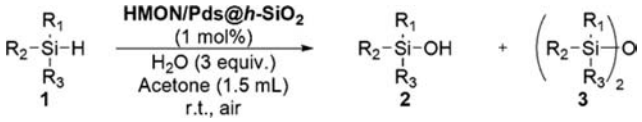

entry	silane (**1**)	time [h]	conv. [%][b]	yield [%][b,c]	TOF [h^{-1}]
1	Et_3SiH (**1a**)	0.25	95	93 (2)	380
2	$PhMe_2SiH$ (**1b**)	0.25	70	69 (<1)	280
3	**1b**	0.5	>99	98 (1)	
4	**1b** (10th run)[d]	0.5	>99	95 (5)	
5	Ph_2MeSiH (**1c**)	0.25	62	60 (2)	248
6[e]	Ph_3SiH (**1d**)[f]	3	>99	98(2)[g]	17

[a]Condition: **1** (0.5 mmol), H_2O (1.5 mmol), acetone (1.5 mL), **HMON/Pds@*h*-SiO$_2$** (1 mol %, based on Pd contents), rt, under air. [b]Determined by GC. [c]Nnumbers in parentheses represent the yield of the product **3**. [d]Recovered catalyst was used in iterative cycles. [e]2 mol % catalyst was used. [f]Conversion was not observed during the reaction with 1 mol % catalyst for 0.25 h. [g]Isolation yield.

explanation requires further research, such a remarkable catalytic activity can be ascribed to both the ultrafine size and the large number of catalytic nanoparticles that are well dispersed on the Mn_3O_4 support layer and the possible synergistic support-catalyst interaction at the Mn_3O_4-Pd heterojunction. Reuse of the recovered **HMON/Pds@*h*-SiO$_2$** in 10 consecutive runs did not lead to any significant decline in its catalytic activity in terms of conversion yield and selectivity, indicating the high recyclability of the hollow nanoreactor carrying the immobilized catalyst system inside the cavity (entry 4). The high dispersion stability of the Mn_3O_4-immobilized Pd nanocrystals, presumably resulting from the strong metal-support interaction, was also confirmed by treating solid **HMON/Pds@*h*-SiO$_2$** at high temperatures; the initial highly dispersed state was retained even after annealing *in vacuo* at 200 °C for 12 h (Figure S6). The catalytic turnover frequency (TOF) of the **HMON/Pds@*h*-SiO$_2$** for the oxidation of **1b** was estimated to be 280 h^{-1} based on 70% of conversion yield during the reaction for 15 min (entry 2). Compared with this, the same reaction with triethylsilane (**1a**) and diphenylmethylsilane (**1c**) gave TOFs of 380 and 248 h^{-1}, respectively (entries 1 and 5). In case of the triphenylsilane (**1d**), the TOF was derived to be only 17 h^{-1} from the reaction performed with 2 mol % catalyst for 3 h (entry 6). The measured TOF values show good correlation with the molecular size of the substrate hydrosilane molecules, indicating that the catalytic conversion inside the hollow cavity of **HMON/Pds@*h*-SiO$_2$** is largely influenced by the diffusion rate of the substrate molecules through the pores of the silica shell.[16] Control reactions using **Mn$_3$O$_4$@Pds**, in which Pd nanocrystals are immobilized on the **Sf-MON** surface, showed the quantitative transformations of **1a**∼**c** and **1d** within 12 and 40 min, respectively. This result evidences the crucial role of the porous silica shell in enhancing the substrate selectivity of the hollow nanoreactor by sorting the substrates according to molecular size. On the other hand, in the experiments to investigate the TON by using 0.0005 mol % of the catalyst, the Pd nanocrystals immobilized in the **Mn$_3$O$_4$@Pds** were found to be aggregated and sintered into larger particles, while any change was detected from the Pd nanocrystals immobilized inside the cavity of the retrieved **HMON/Pds@*h*-SiO$_2$** after the catalytic reaction (Figure S7).

To examine the possibility of expanding the current procedure to a broader range of catalytic species besides Pd and Pt, further investigation was performed on the metal growth with **Sf-MON**. Immersion of **Sf-MON** in $IrCl_3$ and $RhCl_3$ solutions resulted in the formation of Ir and Rh nanocrystals, respectively, on the **Sf-MON** surface, similar to Pd and Pt deposition through the galvanic replacement process. In addition to the monometallic nanocrystals, their alloys such as binary Pd/Pt and quaternary Pd/Pt/Ir/Rh could be deposited by treating **Sf-MON** with solutions containing the corresponding precursor mixtures. The resultant nanocomposites, which immobilize the monometallic and alloy nanocrystals on the **Sf-MON** surface, were identified by using TEM, HR-TEM, and STEM elemental mapping (Figures S8 and S9). Following the successful validation of the extendibility of the galvanic replacement process, we investigated the possible decoration of the hollow nanoreactor with various catalytic species. The reactions of **HMON@*h*-SiO$_2$** with Na_2PtCl_4, $IrCl_3$, and $RhCl_3$ solutions resulted in the growth of Pt, Ir, and Rh nanocrystals with sizes of 1.9 (±0.4), 1.5 (±0.2), and 1.5 (±0.3) nm, respectively, on the Mn_3O_4 layer inside the cavity (Figure 2).

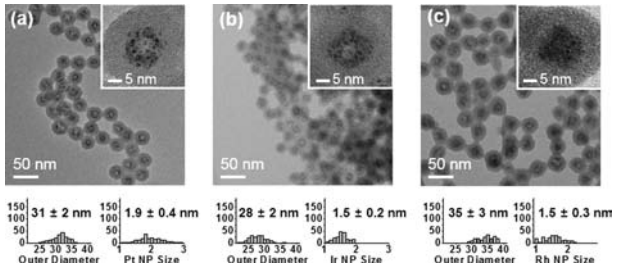

Figure 2. TEM and HRTEM (inset) images of (a) **HMON/Pts@*h*-SiO$_2$**, (b) **HMON/Irs@*h*-SiO$_2$**, and (c) **HMON/Rhs@*h*-SiO$_2$**. Histograms show the outer diameter and the size of the deposited metal nanocrystals.

The resulting **HMON/Ms@*h*-SiO$_2$** (M = Pt, Ir, and Rh) had a functionalized interior surface with a high density of catalytic nanocrystals. Furthermore, hollow nanoreactors, which incorporate alloy nanocrystals such as Pd/Pt and Pd/Pt/Rh/Ir in the hollow interior surface, were successfully fabricated by treating **HMON@*h*-SiO$_2$** in the solutions of the precursor complexes (Figure 3).

In summary, a postsynthetic method for functionalizing preformed hollow nanoparticles with catalytically active metal nanocrystals was developed based on galvanic replacement on the Mn_3O_4 surface inside the cavity. Our method produced hollow nanoreactor systems, in which a high density of ultrafine catalyst nanocrystals are dispersively immobilized on the Mn_3O_4-coated interior surface enclosed by a selectively permeable silica shell. The high effectiveness of the fabricated nanoreactor was demonstrated in terms of its activity, selectivity, and recyclability in catalyzing the silane oxidation reaction. Furthermore, we demonstrated that the procedure explored in this study could be extended into a generalized protocol that is applicable for optimizing and diversifying the functionality of the hollow nanoreactor by combinatorial integration of a wide range of catalytic species inside the cavity.

dx.doi.org/10.1021/ja4083792 | J. Am. Chem. Soc. 2013, 135, 15714−15717

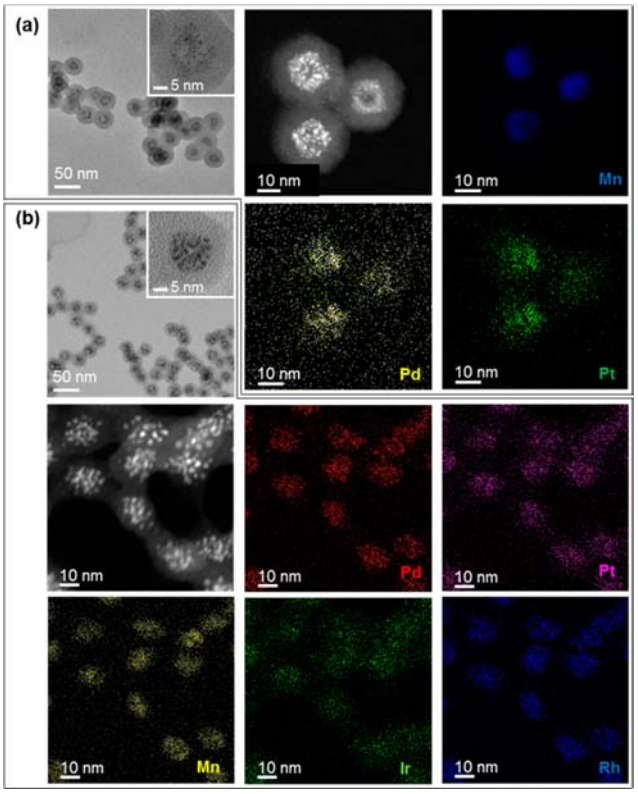

Figure 3. TEM, HRTEM (inset in the left image), and STEM-HAADF images and elementary maps of (a) **HMON/Pd/Pts@*h*-SiO$_2$** and (b) **HMON/Pd/Pt/Rh/Irs@*h*-SiO$_2$**.

■ ASSOCIATED CONTENT

Supporting Information

Experimental details and additional analyses data. This material is available free of charge via the Internet at http://pubs.acs.org.

■ AUTHOR INFORMATION

Corresponding Author

insulee97@postech.ac.kr

Notes

The authors declare no competing financial interest.

■ ACKNOWLEDGMENTS

This work was supported by the National Research foundation of Korea (KRF) grant funded by the Korea government (MEST) (2011-0017377). We thank Dr. N.-S. Lee at POSTECH NCNT for TEM analyses.

■ REFERENCES

(1) Hollow inorganic nanoparticles: (a) Hu, J.; Chen, M.; Fang, X.; Wu, L. *Chem. Soc. Rev.* **2011**, *40*, 5472. (b) Zhang, Q.; Wang, W.; Goebl, J.; Yin, Y. *Nano Today* **2009**, *4*, 494. (c) Lou, X. W.; Archer, L. A.; Yang, Z. *Adv. Mater.* **2008**, *20*, 3987.

(2) (a) Lian, J.; Xu, Y.; Lin, M.; Chan, Y. *J. Am. Chem. Soc.* **2012**, *134*, 8754. (b) Xiao, M.; Zhao, C.; Chen, H.; Yang, B.; Wang, J. *Adv. Funct. Mater.* **2012**, *22*, 4526. (c) Wang, L.; Shi, J.; Zhu, Y.; He, Q.; Xing, H.; Zhou, J.; Chen, F.; Chen, Y. *Langmuir* **2012**, *28*, 4920. (d) Yeo, K. M.; Choi, S.; Anisur, R. M.; Kim, J.; Lee, I. S. *Angew. Chem., Int. Ed.* **2011**, *50*, 745. (e) Tan, L.; Chen, D.; Liu, H.; Tang, F. *Adv. Mater.* **2010**, *22*, 4885.

(3) (a) Cheng, K.; Sun, S. *Nano Today* **2010**, *5*, 183. (b) Tang, S.; Huang, X.; Chen, X.; Zheng, N. *Adv. Funct. Mater.* **2010**, *20*, 2442. (c) Liu, J.; Qiao, S. Z.; Hartono, S. B.; Lu, G. Q. *Angew. Chem., Int. Ed.* **2010**, *49*, 4981.

(4) (a) Xia, Y.; Li, W.; Cobley, C. M.; Chen, J.; Xia, X.; Zhang, Q.; Yang, M.; Cho, E. C.; Brown, P. K. *Acc. Chem. Res.* **2011**, *44*, 914. (b) Chen, Y.; Chen, H.; Zeng, D.; Tian, Y.; Chen, F.; Feng, J.; Shi, J. *ACS Nano* **2010**, *4*, 6001. (c) Shin, J.; Anisur, R. M.; Ko, M. K.; Im, G. H.; Lee, J. H.; Lee, I. S. *Angew. Chem., Int. Ed.* **2009**, *48*, 321.

(5) (a) Wang, Z.; Zhou, L.; Lou, X. W. *Adv. Mater.* **2012**, *24*, 1903. (b) Koo, B.; Xiong, H.; Slater, M. D.; Prakapenka, V. B.; Balasubramanian, M.; Podsiadlo, P.; Johnson, C. S.; Rajh, T.; Shevchenko, E. V. *Nano Lett.* **2012**, *12*, 2429. (c) Wang, B.; Chen, J. S.; Wu, H. B.; Wang, Z.; Lou, X. W. *J. Am. Chem. Soc.* **2011**, *133*, 17146.

(6) Hollow nanoparticle-based catalytic systems: (a) Fang, X.; Zhao, X.; Fang, W.; Chen, C.; Zheng, N. *Nanoscale* **2013**, *5*, 2205. (b) Li, X.; Yang, Y.; Yang, Q. *J. Mater. Chem. A* **2013**, *1*, 1525.

(7) (a) Liu, J.; Yang, H. Q.; Kleitz, F.; Chen, Z. G.; Yang, T.; Strounina, E.; Lu, G. Q.; Qiao, S. Z. *Adv. Funct. Mater.* **2012**, *22*, 591. (b) Yang, Y.; Liu, X.; Li, X.; Zhao, J.; Bai, S.; Liu, J.; Yang, Q. *Angew. Chem., Int. Ed.* **2012**, *51*, 9164. (c) Lee, I.; Joo, J. B.; Yin, Y.; Zaera, F. *Angew. Chem., Int. Ed.* **2011**, *50*, 10208. (d) Guo, L.; Cui, X.; Li, Y.; He, Q.; Zhang, L.; Bu, W.; Shi, J. *Chem. Asian J.* **2009**, *4*, 1480. (e) Arnal, P. M.; Comotti, M.; Schüth, F. *Angew. Chem., Int. Ed.* **2006**, *45*, 8224. (f) Ikeda, S.; Ishino, S.; Harada, T.; Okamoto, N.; Sakata, T.; Mori, H.; Kuwabata, S.; Torimoto, T.; Matsumura, M. *Angew. Chem., Int. Ed.* **2006**, *45*, 7063.

(8) (a) Chen, Y.; Chen, H.; Guo, L.; He, Q.; Chen, F.; Zhou, J.; Feng, J.; Shi, J. *ACS Nano* **2010**, *4*, 529. (b) Liu, B.; Zeng, H. C. *Small* **2005**, *1*, 566. (c) Yin, Y.; Rioux, R. M.; Erdonmez, C. K.; Hughes, S.; Somorjai, G. A.; Alivisatos, A. P. *Science* **2004**, *304*, 711. (d) Sun, Y.; Wiley, B.; Li, Z.−Y.; Xia, Y. *J. Am. Chem. Soc.* **2004**, *126*, 9399.

(9) Yolk-shell nanoparticles: Liu, J.; Qiao, S. Z.; Chen, J. S.; Lou, X. W.; Xing, X.; Lu, G. Q. *Chem. Commun.* **2011**, *47*, 12578.

(10) Kim, K. W.; Kim, S. M.; Choi, S.; Kim, J.; Lee, I. S. *ACS Nano* **2012**, *6*, 5122.

(11) (a) Liu, B.; Zhang, W.; Feng, H.; Yang, X. *Chem. Commun.* **2011**, *47*, 11727. (b) Chen, Z.; Cui, Z.−M.; Niu, F.; Jiang, L.; Song, W.−G. *Chem. Commun.* **2010**, *46*, 6524. (c) Lou, X. W.; Yuan, C.; Rhoades, E.; Zhang, Q.; Archer, L. A. *Adv. Funct. Mater.* **2006**, *16*, 1679.

(12) Anisur, R. M.; Shin, J.; Choi, H. H.; Yeo, K. M.; Kang, E. J.; Lee, I. S. *J. Mater. Chem.* **2010**, *20*, 10615.

(13) (a) Teng, Z.; Su, X.; Zheng, Y.; Sun, J.; Chen, G.; Tian, C.; Wang, J.; Li, H.; Zhao, Y.; Lu, G. *Chem. Mater.* **2013**, *25*, 98. (b) Wang, Q.; Liu, Y.; Yan, H. *Chem. Commun.* **2007**, 2339.

(14) (a) Agostini, G.; Groppo, E.; Piovano, A.; Pellegrini, R.; Leofanti, G.; Lamberti, C. *Langmuir* **2010**, *26*, 11204. (b) Geus, J. W.; van Dillen, A. J. Preparation of Supported Catalysts by Deposition-Precipitation. In *Handbook of Heterogeneous Catalysis*; Ertl, G.; Knözinger, H.; Weitkamp, J., Eds.; VCH: Weinheim, 1997; Vol. *1*, pp 240−257.

(15) (a) Jeon, M.; Han, J.; Park, J. *ChemCatChem* **2012**, *4*, 521. (b) Shimizu, K.; Kubo, T.; Satsuma, A. *Chem.—Eur. J.* **2012**, *18*, 2226. (c) Chung, M.−K.; Orlova, G.; Goddard, J. D.; Schlaf, M.; Harris, R.; Beveridge, T. J.; White, G.; Hallett, F. R. *J. Am. Chem. Soc.* **2002**, *124*, 10508.

(16) (a) Lee, J.; Park, J. C.; Bang, J. U.; Song, H. *Chem. Mater.* **2008**, *20*, 5839. (b) Ikeda, S.; Ikoma, Y.; Kobayashi, H.; Harada, T.; Torimoto, T.; Ohtani, B.; Matsumura, M. *Chem. Commun.* **2007**, 3753.